３．動物実験での脳内輸送の検討

PTD３融合タンパク質（Mycタグ付加）をマウスに腹腔内投与して脳までの輸送状態を調べた。具体的には 50mg/Kg の PTD3-Myc タンパク質を腹腔内に投与して投与後 12 時間までに脳を灌流固定し mycタグに対する抗体を用いて免疫染色を行いで組織での PTD3 融合タンパク質の脳内分布を調べた。血管床末梢辺縁部（A，B）、皮質（C，D）、ＣＡＩ（E，F）のいずれにおいても PTD3 融合タンパク質を投与したネズミでは融合タンパク質（濃茶色）が確認された（図 4）。これらの結果は、腹腔内投与された PTD3 融合タンパク質が血液脳関門を通過し、脳にまでデリバリーされたことを示している。

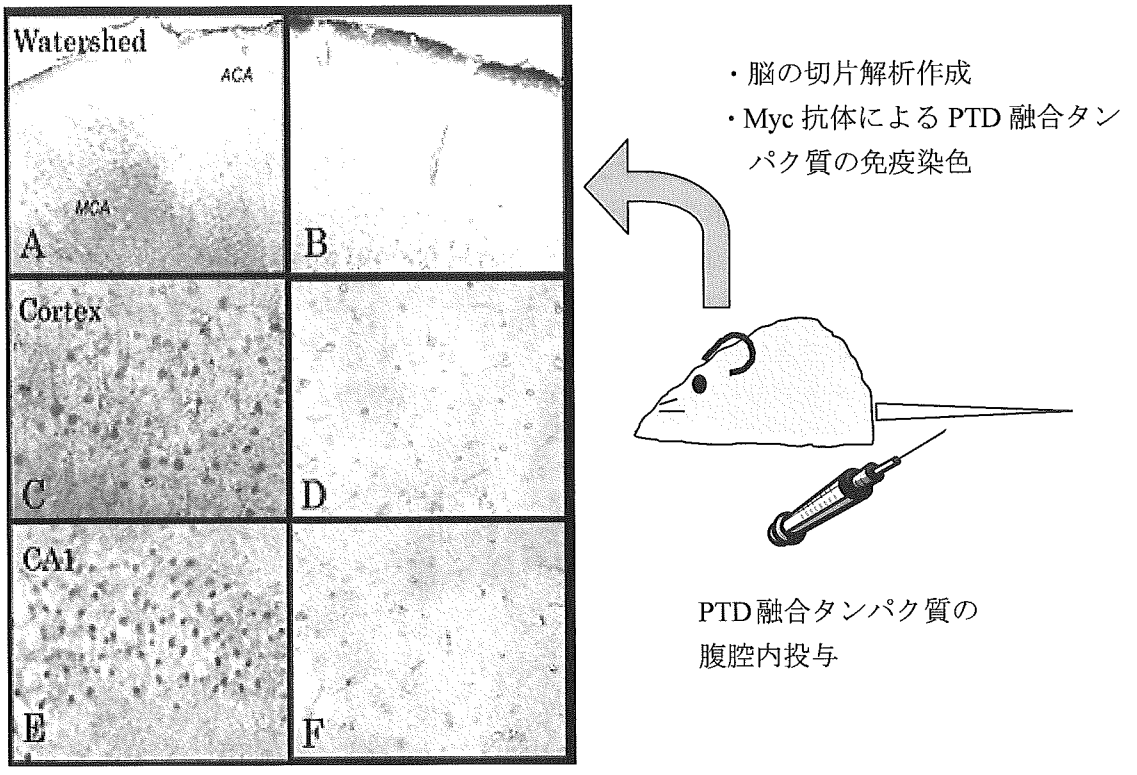

図 4　PTD3 融合タンパク質の脳への移行

A で色のついている領域（MCA;中大脳動脈）は灌流域。ACA（前大脳動脈）灌流域と両者の境界域（Watershed）は PTD 融合タンパク質の染色を認めない。C は MCA 領域の大脳皮質の強拡大、E は海馬 CA1 領域の強拡大でいずれも細胞質・核への取り込みが認められる。B,D,F はそれぞれ A,C,E に対応し、いずれも PTD 融合タンパク質の染色が認められない。

C．研究結果

今年度は、中空バイオナノ粒子を脳に導入するための準備段階という位置づけで研究を行った。

上記のような研究方法により得られた結果から、

1．「PTD の設計とモデルタンパク質の構築」では、リジンとトリプトファンを組み合わせた新規PTD配列を持ったPTD３融合タンパク質を構築することができた。

2．「培養細胞を用いた PTD 融合タンパク質の細胞内輸送の検証」では、構築したPTD３融合タンパク質が効率に細胞内にPTD融合タンパク質を導入でき、融合したタンパク質の機能を発揮できることが分かった。

3．「動物実験での脳内輸送の検討」では、構築したPTD３融合タンパク質をネズミの腹腔内に投与することで、血液脳関門を通し、効率よくデリバリーされることがわかった。

4．我々のグループで実際に検証して得られた上記の PTD の情報を基に、PTD３を組み込んだＬ粒子をコードした遺伝子の構築を行った。この遺伝子を中空バイオナノ粒子を生産するグループに提供し、その粒子の作成するPTDを持った中空バイオナノ粒子を用いて、次年度の研究を進める予定である。

D．考察

1．達成度について

新規のPTD配列を用いたPTD融合タンパク質を全身投与で、脳に効率よく移行できた意義は大きいと考えられる。今後 PTD を融合させた中空バイオナノ粒子のデリバリー効率を検討することにより、細胞内または生体内で任意の組織、および脳に中空バイオナノ粒子内に納めた遺伝子、タンパク質、薬剤等をデリバリーすることが出来るように工夫することができると考えられ、新規 DDS を構築するために必要な準備がなされたと言える。

2．今後の展望について

PTD を持った中空バイオナノ粒子を用いて、次のような研究を予定している。

① PTD－中空バイオナノ粒子内にＥＧＦＰ等のレポーター遺伝子を導入し、培養細胞へのレポーター遺伝子の導入をレポーター遺伝子発現でモニターすることにより検証する。

② PTD－中空バイオナノ粒子内にＥＧＦＰ等のレポータータンパク質を導入し、培養細胞へのレポータータンパク質の導入をレポータータンパク質をモニターすることにより検証する。

③ PTD－中空バイオナノ粒子内にＥＧＦＰ等のレポーター遺伝子またはタンパク質を導入し、マウスへのレポーター遺伝子の導入をレポーター遺伝子発現でモニターすることにより検証する。

以上の検証により、中空バイオナノ粒子に PTD を付加することにより、より効率の良いデリバリーや、普遍的なデリバリーが構築できるか否かの検証ができると考えられる。目的通りに PTD－中空バイオナノ粒子に普遍的なデリバリーを付加する事ができれば、DDS 研究に新たな可能性をもった材料を提供することが出来ることになり、多大な貢献ができると期待される。

E．結語

PTD ペプチド自体がデリバリー機能を持つ極めて大きな可能性を持つ DDS 材料として注目されている。これに、中空バイオナノ粒子という運搬能力が優れた DDS 材料を組み合わせることで、より優れた DDS 材料を作り出すことを目指している。本年度の研究により、PTD ペプチドを中空バイオナノ粒子に導入する第一段階が完了した。今後、PTD－中空バイオナノ粒子を

研究材料として検証することで、より目的に近づくことができると考えられる。

G．研究発表

1．論文発表

1) S. Tachiiri, T. Katagiri, T. Tsunoda, N. Oya, M. Hiraoka and Y. Nakamura. Analysis of gene-expression profiles after gamma irradiation of normal human fibroblasts. Int J Radiat Oncol Biol Phys, 2006, 64:272-9.

2) T. Shibata, T. Shibata, Y. Maetani, H. Isoda and M. Hiraoka. Radiofrequency ablation for small hepatocellular carcinoma: prospective comparison of internally cooled electrode and expandable electrode. Radiology, 2006, 238:346-53.

3) N. Oya, K. Sasai, S. Tachiiri, T. Sakamoto, Y. Nagata, T. Okada, S. Yano, T. Ishikawa, T. Uchiyama and M. Hiraoka. Influence of radiation dose rate and lung dose on interstitial pneumonitis after fractionated total body irradiation: acute parotitis may predict interstitial pneumonitis. Int J Hematol, 2006, 83:86-91.

4) T. Okada, Y. Miki, Y. Fushimi, T. Hanakawa, M. Kanagaki, A. Yamamoto, S. Urayama, H. Fukuyama, M. Hiraoka and K. Togashi. Diffusion-tensor fiber tractography: intraindividual comparison of 3.0-T and 1.5-T MR imaging. Radiology, 2006, 238:668-78.

5) H. Harada, S. Kizaka-Kondoh and M. Hiraoka. Antitumor protein therapy; application of the protein transduction domain to the development of a protein drug for cancer treatment. Breast Cancer, 2006, 13:16-26.

6) S. Zhu, T. Mizowaki, Y. Nagata, K. Takayama, Y. Norihisa, S. Yano and M. Hiraoka. Comparison of three radiotherapy treatment planning protocols of definitive external-beam radiation for localized prostate cancer. Int J Clin Oncol, 2005, 10:398-404.

7) Z. Zhang, H. Harada, K. Tanabe, H. Hatta, M. Hiraoka and S. Nishimoto. Aminopeptidase N/CD13 targeting fluorescent probes: synthesis and application to tumor cell imaging. Peptides, 2005, 26:2182-7.

8) C. Yamauchi, M. Mitsumori, Y. Nagata, M. Kokubo, T. Inamoto, K. Mise, H. Kodama and M. Hiraoka. Bilateral breast-conserving therapy for bilateral breast cancer: results and consideration of radiation technique. Breast Cancer, 2005, 12:135-9.

9) K. Takayama, Y. Nagata, Y. Negoro, T. Mizowaki, T. Sakamoto, M. Sakamoto, T. Aoki, S. Yano, S. Koga and M. Hiraoka. Treatment planning of stereotactic radiotherapy for solitary lung tumor. Int J Radiat Oncol Biol Phys, 2005, 61:1565-71.

10) M. Sakamoto, N. Oya, T. Mizowaki, N. Araki, Y. Nagata, K. Takayama, J. A. Takahashi, H. Kano, T. Katsuki, N. Hashimioto and M. Hiraoka. Initial Experiences of Palliative Stereotactic Radiosurgery for Recurrent Brain Lymphomas. J Neurooncol, 2005,

11) H. Sai, M. Mitsumori, N. Araki, T. Mizowaki, Y. Nagata, Y. Nishimura and M. Hiraoka. Long-term results of definitive radiotherapy for stage I esophageal cancer. Int J Radiat Oncol Biol Phys, 2005, 62:1339-44.

12) N. Oya, K. Shibuya, T. Sakamoto, T. Mizowaki, R. Doi, K. Fujimoto, M. Imamura, Y. Nagata and M. Hiraoka. Chemoradiotherapy in Patients with

Pancreatic Carcinoma: Phase-I Study with a Fixed Radiation Dose and Escalating Doses of Weekly Gemcitabine. Pancreatology, 2005, 6:109-116.

13) M. Ogura, T. Shibata, J. Yi, J. Liu, R. Qu, H. Harada and M. Hiraoka. A tumor-specific gene therapy strategy targeting dysregulation of the VHL/HIF pathway in renal cell carcinomas. Cancer Sci, 2005, 96:288-94.

14) T. Nakayama, T. Tsuboyama, J. Toguchida, C. Tanaka, N. Oya, M. Hiraoka and T. Nakamura. Recurrence of osteosarcoma after intraoperative radiation therapy. Orthopedics, 2005, 28:1195-7.

15) Y. Nagata, K. Takayama, Y. Matsuo, Y. Norihisa, T. Mizowaki, T. Sakamoto, M. Sakamoto, M. Mitsumori, K. Shibuya, N. Araki, S. Yano and M. Hiraoka. Clinical outcomes of a phase I/II study of 48 Gy of stereotactic body radiotherapy in 4 fractions for primary lung cancer using a stereotactic body frame. Int J Radiat Oncol Biol Phys, 2005, 63:1427-31.

16) M. Mitsumori, M. Hiraoka, Y. Negoro, C. Yamauchi, N. Shikama, S. Sasaki, T. Yamamoto, T. Teshima and T. Inoue. The patterns of care study for breast-conserving therapy in Japan: analysis of process survey from 1995 to 1997. Int J Radiat Oncol Biol Phys, 2005, 62:1048-54.

17) Lyshchik, T. Higashi, R. Asato, S. Tanaka, J. Ito, J. J. Mai, C. Pellot-Barakat, M. F. Insana, A. B. Brill, T. Saga, M. Hiraoka and K. Togashi. Thyroid gland tumor diagnosis at US elastography. Radiology, 2005, 237:202-11.

18) Lyshchik, T. Higashi, R. Asato, S. Tanaka, J. Ito, M. Hiraoka, A. B. Brill, T. Saga and K. Togashi. Elastic moduli of thyroid tissues under compression. Ultrason Imaging, 2005, 27:101-10.

19) J. Liu, R. Qu, M. Ogura, T. Shibata, H. Harada and M. Hiraoka. Real-time imaging of hypoxia-inducible factor-1 activity in tumor xenografts. J Radiat Res (Tokyo), 2005, 46:93-102.

20) H. Harada, S. Kizaka-Kondoh and M. Hiraoka. Optical imaging of tumor hypoxia and evaluation of efficacy of a hypoxia-targeting drug in living animals. Mol Imaging, 2005, 4:182-93.

21) Oka S, Masutani H, Liu W, Horita H, Wang D, Kizaka-Kondoh S, Yodoi J. Thioredoxin-binding protein-2 (TBP-2)-like inducible membrane protein (TLIMP) is a novel Vitamin D3- and PPAR-ã ligand target protein that regulates PPAR-ã signal. *Endocrinology*. 147(2):733-743 (2006).

22) Y Kageyama, H Sugiyama, H Ayame, A Iwai, Y Fujii, L Eric Huang, Kizaka-Kondoh S, Hiraoka M. and. Kihara K. Suppression of VEGF transcription in renal cell carcinoma cells using pyrrole-imidazole hairpin polyamides targeting the hypoxia responsive element. *Acta Oncologica.* In press.

23) 近藤科江、原田浩、平岡真寛。革新的診断・治療へのアプローチ；膜透過性・標的特異性を有する融合タンパク質を用いたイメージング、ターゲティング。BioClinica 20(1), 53-58. 2005

24) 近藤科江、平岡真寛、原田浩。がん治療における HIF-1 と Tumor Hypoxia. Cancer Frontier 7: 77-86. 2005

25) 近藤科江。 Meeting Report がん分子標的治療研究会総会 がん分子標的治療 4(1), 62-64. 2006.

26) 近藤科江、原田浩、平岡真寛。『低酸素がん細胞』を標的としたがんのイメージング・ターゲティング バイオテクノロジージャーナル 6 (2), 234-237. 2006.
27) 近藤科江、原田浩、平岡真寛。低酸素を標的とした生体イメージング分子プローブの開発。未来医学。印刷中

２．学会発表

1) S. Kizaka-Kondoh, H. Harada, X. Xie, S. Itasaka, K. Shibuya, M. Hiraoka. Optical Imaging of HIF-1 activity in malignant solid tumors for evaluation of cancer therapies, Molecular Imaging, 4(3), 324, 2005. (Forth Annual Meeting, Cologne, Germany, September 7-10, 2005)

H．知的財産権の出願・登録状況

国際出願番号：PCT/JP2006/304701
発明の名称：病態の状態をリアルタイムで観察可能なモデル動物とそれを可能にする遺伝子構築物及びその使用

1) 発明者:近藤科江、原田浩、平岡真寛、山田秀一
2) 出願日：2006 年 3 月 10 日
3) 出願人：京都大学、関西ＴＬＯ

研究成果の刊行に関する一覧表

発表者氏名	論文タイトル名	発表誌名	巻号	ページ	出版年
Yu, D., Amano, C., Fukuda, T., Yamada, T., Kuroda, S., Tanizawa, K., Kondo, A., Ueda, M., Yamada, H., Tada, H., and Seno, M	The Specific Delivery of Proteins to Human Liver Cells by Engineered Bio-Nanocapsules.	FEBS J.	272(14)	3651-3660	2005
近藤昭彦、黒田俊一、谷澤克行、妹尾昌治、上田政和	革新的なナノキャリア：中空バイオナノ粒子によるピンポイントDDS	月刊「バイオインダストリー」	22, No. 5	22-27	2005
近藤昭彦、黒田俊一、谷澤克行、妹尾昌治、上田政和	中空バイオナノ粒子を用いたピンポイントDDSの開発	月刊「ケミカル・エンジニヤリング」	50, No. 5	23-28	2005
山田忠範、妹尾昌治、上田政和、近藤昭彦、谷澤克行、黒田俊一	細胞及び組織特異的遺伝子導入を可能にするバイオナノカプセル	生物工学会会誌	83, No. 8	380-383	2005
近藤昭彦	創薬などに期待高まる「細胞表層工学」	日経ナノビジネス	9	20-23	2005
鄭周姫、黒田俊一	ナノテクが導く「効果的な遺伝子治療」	月刊「化学」	60, No. 1	23-25	2005
黒田俊一	バイオナノカプセルが拓く新しい医療技術	バイオサイエンスとインダストリー	63, No. 9	589-590	2005
黒田俊一	バイオナノカプセルの開発と化粧品への応用	Fragrance Journal	No. 11	22-28	2005
Yamada S, Terada K, Ueno Y, Sugiyama T, Seno M, Kojima I.	Differentiation of adult hepatic stem-like cells into pancreatic endocrine cells.	Cell Transplant	14(9)	647-653	2005
Tuoya, Hirayama K, Nagaoka T, Yu D, Fukuda T, Tada H, Yamada H, Seno M.	Identification of cell surface marker candidates on SV-T2 cells using DNA microarray on DLC-coated glass.	Biochem Biophys Res Commun	19;334(1)	263-268	2005

Ogata T, Dunbar AJ, Yamamoto Y, Tanaka Y, Seno M, Kojima I	Betacellulin-delta4, a novel differentiation factor for pancreatic beta-cells, ameliorates glucose intolerance in streptozotocin-treated rats.	Endocrinology	146(11)	4673-4681	2005
Kitazoe M, Murata H, Futami J, Maeda T, Sakaguchi M, Miyazaki M, Kosaka M, Tada H, Seno M, Huh NH, Namba M, Nishikawa M, Maeda Y, Yamada H.	Protein transduction assisted by polyethylenimine-cationized carrier proteins.	J Biochem	137(6)	693-701	2005
Hayashida T, Ueda M, Aiura K, Tada H, Onizuka M, Seno M, Yamada H, Kitajima M.	Anti-angiogenic effect of an insertional fusion protein of human basic fibroblast growth factor and ribonuclease-1.	Protein Eng Des Sel	18(7)	321-327	2005
Futami J, Kitazoe M, Maeda T, Nukui E, Sakaguchi M, Kosaka J, Miyazaki M, Kosaka M, H Tada, Seno M, Sasaki J, Hhuh N, Namba M, Yamada H	Intracellular delivery of proteins into mammalian living cells by polyethyleneimine-cationization.	J Biosci Bioeng.	99 (2)	95-103	2005
Nakamura T., Ozawa S., Kitagawa Y., Ueda M., Kubota T., Kitajima M	Antianggiogenic agent SU6668 suppresses the tumor growth of xenografted A431 cills.	Oncology Rep	15	79-83	2006
Akatsu T., Ueda M., Shimazu M., Wakabayashi G., Aiura K., Tanabe M., Kawachi S., Kameyama K., Kitajima M.	Primary undifferentiated spindle-cell carcinoma of the gallbladder presenting as a liver tumor.	J.Gastroenterol	40	993-998	2005
Kawakubo H., Ozawa S.., Ando N., Kitagawa Y., Mukai M., Ueda M., Kitajima M.	Alterations of p53,cyclin D1 and pRB expression in the carcinogenesis of esophageal squamous cell carcinoma.	Oncology Rep	14	1453-1459	2005

Akatsu T., Ueda M., Shimazu M., Wakabayashi G., Aiura K., Tanabe M., Kawachi S., Kido H., Kitajima M.	Long-term survival of patients with gallbladder cancer detected during or after laproscopic cholecystectomy.	World J Surg.	29	1106-1109	2005
Nakamura T., Ozawa S., Kitagawa Y., Shin C-H., Ueda M., Kitajima M.	Expression of basic fibroblast growth factor is associated with a good outcome in patients with squamous cell carcinoma of the esophagus.	Oncology Rep	14	617-623	2005
Hoshimoto S., Aiura K.., Suzuki M., Ueda M., Kitajiam M., Kameyama K., Mukai M.	Resection of pancreatic metastases originating from papillary carcinoma of the thyroid A case report.	Pancreas	31(1)	8	2005
Akatsu T., Shimazu M., Kawachi S., Tanabe M., Aiura K., Wakabayashi G., Ueda M., Sakamoto M., Kitajima M.	Long-term survival of intrahepatic cholangiocarcinoma with hilar lymph node metastasis and portal vein involvement.	Hepato-Gastroenterology	52	603-605	2005
Hayashida T., Ueda M., Aiura K., Tada H., Onizuka M., Seno M., Yamada H.,Kitajima M.	Anti-angiogenic effect of an insertional fusion protein of human basic fibroblast growth factor and ribonuclease-1.	Protein Engineering, Design & Selection	18(7)	321-327	2005
Imai E., Ueda M., Kanao K., Miyaki K., Kubota T., Kitajima M.	Surgical site infection surveillance after open gastrectomy and risk factors for surgical site infection.	J Infect Chemother	11	141-145	2005
Miyata R., Shimazu M., Kawachi S., Tanabe M., Aiura K., Wakabayashi G., Ueda M., Sakamoto M., Kitajima M.	Left tgrisegmentectomy and combined resection of the inferior vena cava, without reconstruction, for giant cystadenocarcinoma of the liver	J Heptobiliary pancreat Surg	12	272-276	2005

Akatsu T., Yoshida M., Kubota T., Shimazu M., Ueda M., Otani Y., Wakabayashi G., Aiura K., Tanabe M., Furukawa T., Saikawa Y., Kawachi S, Akatsu Y., Kitajima M.	Gallstone disease after extended(d2) lymph node dissection for gastric cancer.	World J Surg.	29(2)	182-186	2005
Akatsu T., Ueda M., Shimazu M., Kawachi S., Tanabe M., Aiura K., Wakabayashi G., Sakamoto M., Matsuo R., Kitajima M.	Spontaneous rupture of a mass-forming type peripheral cholangioacrcinoma.	J. Gasteroenterol Hepatol	20(1)	162-163	2005
S. Tachiiri, T. Katagiri, T. Tsunoda, N. Oya, M. Hiraoka and Y. Nakamura.	Analysis of gene-expression profiles after gamma irradiation of normal human fibroblasts.	Int J Radiat Oncol Biol Phys	64	272-279	2006
T. Shibata, T. Shibata, Y. Maetani, H. Isoda and M. Hiraoka.	Radiofrequency ablation for small hepatocellular carcinoma: prospective comparison of internally cooled electrode and expandable electrode.	Radiology	238	346-353	2006
N. Oya, K. Sasai, S. Tachiiri, T. Sakamoto, Y. Nagata, T. Okada, S. Yano, T. Ishikawa, T. Uchiyama and M. Hiraoka.	Influence of radiation dose rate and lung dose on interstitial pneumonitis after fractionated total body irradiation: acute parotitis may predict interstitial pneumonitis.	Int J Hematol	83	86-91	2006
T. Okada, Y. Miki, Y. Fushimi, T. Hanakawa, M. Kanagaki, A. Yamamoto, S. Urayama, H. Fukuyama, M. Hiraoka and K. Togashi.	Diffusion-tensor fiber tractography: intraindividual comparison of 3.0-T and 1.5-T MR imaging.	Radiology	238	668-678	2006
H. Harada, S. Kizaka-Kondoh and M. Hiraoka.	Antitumor protein therapy; application of the protein transduction domain to the development of a protein drug for cancer treatment.	Breast Cancer	13	16-26	2006

S. Zhu, T. Mizowaki, Y. Nagata, K. Takayama, Y. Norihisa, S. Yano and M. Hiraoka.	Comparison of three radiotherapy treatment planning protocols of definitive external-beam radiation for localized prostate cancer.	Int J Clin Oncol	10	398-404	2005
Z. Zhang, H. Harada, K. Tanabe, H. Hatta, M. Hiraoka and S. Nishimoto.	Aminopeptidase N/CD13 targeting fluorescent probes: synthesis and application to tumor cell imaging.	Peptides	26	2182-2187	2005
C. Yamauchi, M. Mitsumori, Y. Nagata, M. Kokubo, T. Inamoto, K. Mise, H. Kodama and M. Hiraoka.	Bilateral breast-conserving therapy for bilateral breast cancer: results and consideration of radiation technique.	Breast Cancer	12	135-139	2005
K. Takayama, Y. Nagata, Y. Negoro, T. Mizowaki, T. Sakamoto, M. Sakamoto, T. Aoki, S. Yano, S. Koga and M. Hiraoka.	Treatment planning of stereotactic radiotherapy for solitary lung tumor.	Int J Radiat Oncol Biol Phys	61	1565-1571	2005
M. Sakamoto, N. Oya, T. Mizowaki, N. Araki, Y. Nagata, K. Takayama, J. A. Takahashi, H. Kano, T. Katsuki, N. Hashimioto and M. Hiraoka.	Initial Experiences of Palliative Stereotactic Radiosurgery for Recurrent Brain Lymphomas.	J Neurooncol			2005
H. Sai, M. Mitsumori, N. Araki, T. Mizowaki, Y. Nagata, Y. Nishimura and M. Hiraoka.	Long-term results of definitive radiotherapy for stage I esophageal cancer.	Int J Radiat Oncol Biol Phys	62	1339-1344	2005
N. Oya, K. Shibuya, T. Sakamoto, T. Mizowaki, R. Doi, K. Fujimoto, M. Imamura, Y. Nagata and M. Hiraoka.	Chemoradiotherapy in Patients with Pancreatic Carcinoma: Phase-I Study with a Fixed Radiation Dose and Escalating Doses of Weekly Gemcitabine.	Pancreatology	6	109-116	2005
M. Ogura, T. Shibata, J. Yi, J. Liu, R. Qu, H. Harada and M. Hiraoka.	A tumor-specific gene therapy strategy targeting dysregulation of the VHL/HIF pathway in renal cell carcinomas.	Cancer Sci	96	288-294	2005

T. Nakayama, T. Tsuboyama, J. Toguchida, C. Tanaka, N. Oya, M. Hiraoka and T. Nakamura.	Recurrence of osteosarcoma after intraoperative radiation therapy.	Orthopedics	28	1195-1197	2005
Y. Nagata, K. Takayama, Y. Matsuo, Y. Norihisa, T. Mizowaki, T. Sakamoto, M. Sakamoto, M. Mitsumori, K. Shibuya, N. Araki, S. Yano and M. Hiraoka.	Clinical outcomes of a phase I/II study of 48 Gy of stereotactic body radiotherapy in 4 fractions for primary lung cancer using a stereotactic body frame.	Int J Radiat Oncol Biol Phys	63	1427-1431	2005
M. Mitsumori, M. Hiraoka, Y. Negoro, C. Yamauchi, N. Shikama, S. Sasaki, T. Yamamoto, T. Teshima and T. Inoue.	The patterns of care study for breast-conserving therapy in Japan: analysis of process survey from 1995 to 1997.	Int J Radiat Oncol Biol Phys	62	1048-1054	2005
Lyshchik, T. Higashi, R. Asato, S. Tanaka, J. Ito, J. J. Mai, C. Pellot-Barakat, M. F. Insana, A. B. Brill, T. Saga, M. Hiraoka and K. Togashi.	Thyroid gland tumor diagnosis at US elastography.	Radiology	237	202-211	
Lyshchik, T. Higashi, R. Asato, S. Tanaka, J. Ito, M. Hiraoka, A. B. Brill, T. Saga and K. Togashi.	Elastic moduli of thyroid tissues under compression.	Ultrason Imaging	27	101-110	2005
J. Liu, R. Qu, M. Ogura, T. Shibata, H. Harada and M. Hiraoka	Real-time imaging of hypoxia-inducible factor-1 activity in tumor xenografts.	J Radiat Res (Tokyo)	46	93-102	2005
H. Harada, S. Kizaka-Kondoh and M. Hiraoka.	Optical imaging of tumor hypoxia and evaluation of efficacy of a hypoxia-targeting drug in living animals.	Mol Imaging	4	182-193	2005

Oka S, Masutani H, Liu W, Horita H, Wang D, Kizaka-Kondoh S, Yodoi J.	Thioredoxin-binding protein-2 (TBP-2)-like inducible membrane protein (TLIMP) is a novel Vitamin D3- and PPAR-ã ligand target protein that regulates PPAR-ã signal.	*Endocrinology.*	147(2)	733-743	2006
近藤科江、原田浩、平岡真寛	革新的診断・治療へのアプローチ；膜透過性・標的特異性を有する融合タンパク質を用いたイメージング、ターゲティング	BioClinica	20(1)	53-58	2005
近藤科江、平岡真寛、原田浩	がん治療における HIF-1 と Tumor Hypoxia.	Cancer Frontier	7	77-86	2005
近藤科江	Meeting Report がん分子標的治療研究会総会	がん分子標的治療	4(1)	62-64	2006
近藤科江、原田浩、平岡真寛	『低酸素がん細胞』を標的としたがんのイメージング・ターゲティング	バイオテクノロジージャーナル	6 (2)	234-237	2006

the FEBS Journal

The specific delivery of proteins to human liver cells by engineered bio-nanocapsules

Dongwei Yu[1], Chie Amano[1], Takayuki Fukuda[1,2], Tadanori Yamada[3], Shun'ichi Kuroda[3,4], Katsuyuki Tanizawa[3,4], Akihiko Kondo[4,5], Masakazu Ueda[4,6], Hidenori Yamada[1], Hiroko Tada[1] and Masaharu Seno[1,4,7]

1 Graduate School of Natural Science and Technology, Okayama University, Japan
2 Kobe R & D Center, Katayama Chemical Industries Co. Ltd, Kobe, Japan
3 Institute of Scientific and Industrial Research, Osaka University, Japan
4 Research and Development Division, Beacle, Inc., Okayama, Japan
5 Faculty of Engineering, Kobe University, Japan
6 Keio University, School of Medicine, Tokyo, Japan
7 Research Center for Biomedical Engineering, Okayama University, Japan

Keywords
bio-nanocapsule; L fusion protein; protein delivery vector; specific infection; topology

Correspondence
M. Seno, Graduate School of Natural Science and Technology, Okayama University, 3.1.1 Tsushima-Naka, Okayama 700-8530, Japan
Tel/Fax: +81 86 251 8216
E-mail: mseno@cc.okayama-u.ac.jp

(Received 20 March 2005, revised 9 May 2005, accepted 24 May 2005)

doi:10.1111/j.1742-4658.2005.04790.x

A bio-nanocapsule (BNC), composed of the surface antigen (sAg) of the hepatitis B virus, is an efficient nanomachine with which to accomplish the liver-specific delivery of genes and drugs. Approximately 110 molecules of sAg are associated to form a BNC particle with an average diameter of 130 nm. The L protein is an sAg peptide composed mainly of preS and S regions. The preS region, with specific affinity for human hepatocytes, is localized in the N-terminus. The S region following the preS has two transmembrane regions responsible for the formation of particles. In this study, the fusion of emerald green fluorescent protein (EGFP) at the C-terminus of the S region was designed to deliver proteins to human hepatocytes. Truncation of the C-terminus of the S region was required to obtain sufficient expression levels in Cos7 cells. The nanoparticles that were produced delivered EGFP to human hepatoma cells, displaying the EGFP moiety outside, or enclosing it inside. However, only a single orientation characterizes the particle, so that either type of L fusion particle could be effectively and independently separated by an antibody affinity column. The dual C-terminal topologies of the L fusion particles designed in this study could be applied to various proteins for the C-terminal moiety of the L fusion proteins, depending on the character of the proteins, such as cytoplasmic proteins, as well as cytokines or ligands to cell surface receptors. We suggest that this fusion design is the most efficient way to prepare a BNC that delivers proteins to specific cells or tissues.

A drug and gene delivery system has long been considered important for drug discovery and pharmaceutical development. In particular, the establishment of a cell- or tissue-specific targeting method is the latest area of focus. Although, viral vectors, such as those utilizing adenovirus or adeno-associated virus, have been developed for gene therapy, the cell specificity must be ameliorated. Some other problems, such as inflammation, neutralizing antibodies, the dangers of mass production, and insertional mutagenesis, limit the use of

Abbreviations
BNC, bio-nanocapsule; DDS, drug delivery system; DMEM, Dulbecco's modified Eagle's medium; EGFP, emerald green fluorescent protein; ER, endoplasmic reticulum; FBS, fetal bovine serum; HBV, hepatitis B virus; IFN, interferon; PMSF, phenylmethanesulfonyl fluoride; sAg, surface antigen.

viral vectors in humans. By contrast, liposomes as a drug delivery vector have no limits to mass production and do not have the drawbacks of viral vectors. However, liposomes have a lower transfection efficiency and cell/tissue specificity compared with viral vectors, even though they have the ability to transfer proteins into cells. To find a material that has good tranfection efficiency free from the hazards of viral infection, we come up with the idea of using a hollow particle derived from recombinant viral envelope proteins. The hepatitis B virus (HBV) is a human liver-specific virus whose 3.2-kb genome codes three envelope proteins in a single open reading frame (ORF). These encoded surface antigens (sAgs) are called small (S), medium (M) and large (L) proteins [1]. In 1982, Valenzuela *et al.* succeeded in preparing recombinant sAg from yeast as S protein particles with a diameter of 22 nm [2]. Around 1990, recombinant L proteins were also found to be produced in yeast cells as hollow virus-like particles and were developed as immunogens for hepatitis B vaccines, which were proven safe for use in humans [3,4]. The recombinant L proteins formed a virus-like particle with a diameter of approximately 200 nm when produced in *Saccharomyces cerevisiae* [3,5]. We reported that this particle was extremely useful as a vector to target human hepatocyte *in vivo* exploiting the character of infectivity of HBV limited to human liver [6]. Because this recombinant particle is empty, we named this hollow nanoparticle a bio-nanocapsule (BNC) as it represents an efficient nanomachine for achieving liver-specific delivery of genes and drugs.

Although electroporation is proposed as a convenient procedure for enclosing substances in the particle [6], fusion to the C-terminus of L protein appears to be the most efficient way to prepare a BNC to convey foreign proteins. Thus, fusing a suitable protein to the tail should be a convenient way of preparing a BNC that delivers proteins to human hepatocytes.

Results

Evaluation of hepatitis B L fusion particles

The HBV L envelope protein is composed of three major regions. The preS1 region of 108 or 119 amino acids at the N-terminus directly recognizes human hepatocytes [1,7–9]. The preS2 region of 55 amino acids following the preS1 region has an affinity with polymerized albumin-mediated interactions. The major 226 amino acids of the S region occupy the C-terminal half of the L protein. Current models for the transmembrane structure of the S region assume that both the N- and C-termini are at external positions in mature particles [10,11]. Although it is predicted that four transmembrane-like α helices are present in the S region, only the two in the N-terminus have been shown to be transmembrane helices [12–14]. These two domains, which correspond to amino acids 8–22 and 80–98, respectively, are separated by a hydrophilic region that is exposed to the internal side of the mature particle. The C-terminal topology of the S region has not been challenged experimentally and remains to be investigated [12,15], whereas the preS region has been shown to protrude into the lumen of the endoplasmic reticulum (ER) [16]. To enclose protein inside the BNC, we designed emerald green fluorescent protein (EGFP) fusion at the C-terminus of the S region, with or without truncation, using 32, 45 and 54 amino acid residues from the C-terminus, respectively, to obtain four types of L fusion particles, L-FLAG–EGFP, L(Δ32)-FLAG–EGFP, L(Δ45)-FLAG–EGFP and L(Δ54)-FLAG–EGFP, with an intervening sequence of FLAG-tag (Fig. 1). Truncations were designed to shorten the C-terminus as much as possible for a single transmembrane spanning region. Because proline often functions as a helix disruptor, the proline residues at 177 and 187 are considered in the truncation.

According to the amino acid sequence, the molecular mass of L-FLAG–EGFP, which is the fusion protein between the full length of the L protein and EGFP, is calculated to be 68.5 kDa. The apparent molecular mass of L-FLAG–EGFP is 71.5 kDa due to the glycosylated Asn146 in the S region on SDS/PAGE [15,17]. Taking the sizes of C-terminal truncation into account, the molecular mass of each L(Δ32)-FLAG–EGFP, L(Δ45)-FLAG–EGFP and L(Δ54)-FLAG–EGFP is calculated to be 68, 66.5 and 65.7 kDa, respectively.

These L proteins fused to EGFP were transiently expressed in Cos7 cells (Fig. 2A). During the culturing period, EGFP fluorescence was observed from the transfected Cos7 cells along the ER and Golgi, but not in the nuclei, indicating that the fused protein was produced in the secretional path. Fusion proteins were detected with both anti-S and anti-GFP IgG in the cell lysates of transfected cells by western blotting at their expected sizes, as calculated (Fig. 2B). Immunoprecipitates of the conditioned media, with either anti-S, anti-FLAG or anti-GFP IgG, showed bands of fusion proteins, in addition to those in the cell lysates (Fig. 2C). Secretion of L-FLAG–EGFP and L(Δ54)-FLAG–EGFP from Cos7 cells appeared limited, although it was, in fact, produced in sufficient quantity. Expression and secretion of L(Δ32)-FLAG–EGFP were both low. Secretion of L(Δ45)-FLAG–EGFP was obviously the highest of the four fusion constructs.

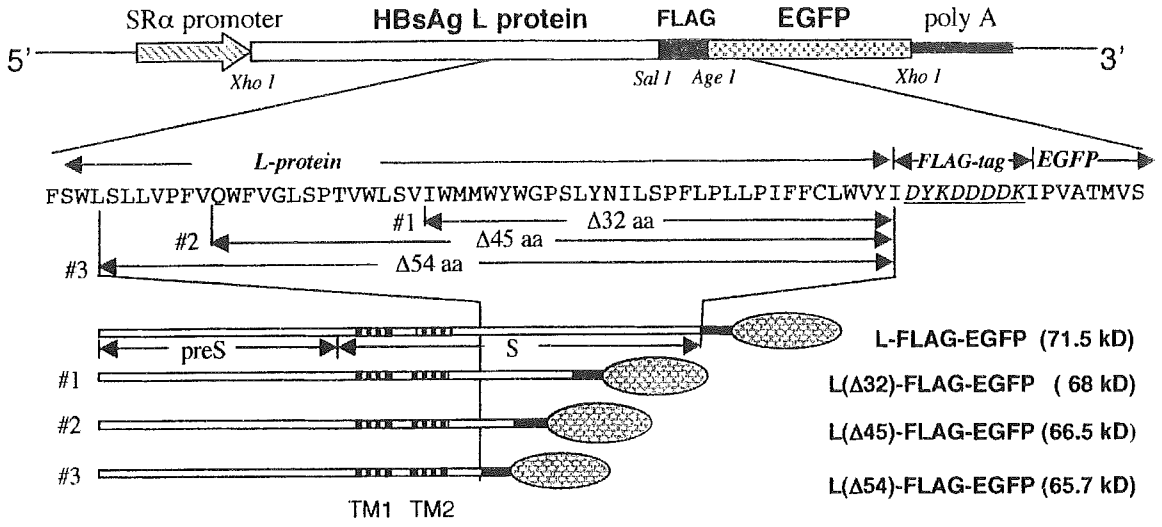

Fig. 1. Fusion proteins between L and EGFP. The 720 bp *egfp* gene was ligated to the 3′ side of the L gene of the hepatitis B virus flanking a 39 bp FLAG as a spacer sequence in an open reading frame. The resultant gene coding L-FLAG–EGFP was inserted downstream of a SRα promoter. The C-terminus of the L protein was truncated by 32 (96 bp), 45 (135 bp) and 54 amino acid residues (162 bp) to optimize expression of the L fusion protein. The resultant fusion proteins are designated as L-FLAG–EGFP, L(Δ32)-FLAG–EGFP, L(Δ45)-FLAG–EGFP, and L(Δ54)-FLAG–EGFP. TM1 and TM2 represent transmembrane regions of the L protein.

The conditioned media were further assessed for the secretion of these different constructs of particles using enzyme immunoassay and fluorescence (Fig. 3). When the level of L-FLAG–EGFP was considered to be 100%, that of L(Δ45)-FLAG–EGFP was > 300% in EIA. The fluorescence from the EGFP moiety of L fusion protein showed that L(Δ45)-FLAG–EGFP was secreted at the highest ratio. The analyses revealed that L(Δ45)-FLAG–EGFP was suitably optimized for production as the fusion protein.

L(Δ45)-FLAG–EGFP particle formation was assessed by sucrose gradient ultracentrifugation (Fig. 4). When cell extracts were subjected to ultracentrifugation, both fluorescence and immunoreactivity were seen in the same fraction at a density of 1.11 $g \cdot mL^{-1}$, whereas the native EGFP fluorescence peak was found to have a density of 1.05 $g \cdot mL^{-1}$. Peak fractions were analyzed by western blotting to confirm the presence of fusion protein at 66.5 kDa. The density of the particles obtained from both cell extracts and the conditioned media was equivalent to that of the BNC. Whether from the conditioned media or the cell extracts, L(Δ45)-FLAG–EGFP has the potential to form a particle.

Topology analysis of the C-terminus of L fusion protein

Consisting of 56 amino acids, the primary structure of the C-terminus of the S region is rich in hydrophobic residues. Therefore, the computer-assisted prediction assumes that there should be two α helices, which traverse the ER membrane twice [11,18]. In this context, EGFP fused to L protein with an intervening FLAG sequence may provide an excellent means of judging the C-terminal topology. Because L-FLAG–EGFP could be immunoprecipitated by anti-FLAG and anti-GFP IgG (Fig. 2C), the L protein C-terminus should be located on the external side of the particle. This is consistent with results reported by Eble *et al.* [12].

Because generation of its fluorophore depends on the correct formation of a tertiary structure and can easily be detected by fluorescence microscopy, EGFP has quickly become a powerful research tool for gene expression and subcellular protein localization in living cells and organisms. It was useful in this study, not only to estimate the level of L-EGFP fusion protein expression, but also to observe the infection of particles by its fluorescence. Within the structure of EGFP, chromophores are insulated by tightly woven barrel formations of β sheets, which offer strong resistance against proteolytic attack [19,20]. This resistance was confirmed by incubation with proteinase K at 60 °C for 6 h (data not shown). As a result of this resistance, a convenient protease protection assay was available to determine the topology of the fused protein, as described below. However, slight digestion after 1 h of incubation was observed, indicating that the terminal sequences might be sensitive to proteinase K (Fig. 5).

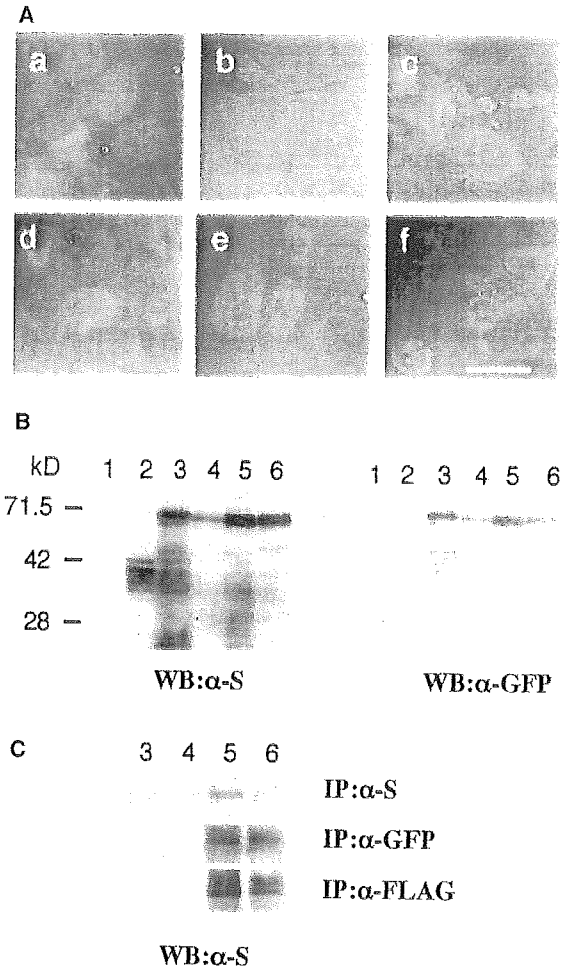

Fig. 2. Expression of L fusion proteins in Cos7 cells. (A) Cells were transfected with plasmids to express (a) EGFP, (b) L protein, (c) L-FLAG–EGFP, (d) L(Δ32)-FLAG–EGFP, (e) L(Δ45)-FLAG–EGFP, and (f) L(Δ54)-FLAG–EGFP, by electroporation. Two days after electroporation, the green fluorescence was observed under a confocal microscope at a 63-fold magnification. The bar scale shows 50 μm. After 3 days, the Cos7 cells were harvested and disrupted by sonication. (B) Cell lysates were probed in western blots with anti-S or anti-GFP IgG. (C) Conditioned media were collected, immunoprecipitated with anti-S, anti-GFP or anti-FLAG IgG, respectively, and subjected to western blotting with anti-S IgG. Lane 1, EGFP; lane 2, L protein; lane 3, L-FLAG–EGFP; lane 4, L(Δ32)-FLAG–EGFP; lane 5, L(Δ45)-FLAG–EGFP; lane 6, L(Δ54)-FLAG–EGFP.

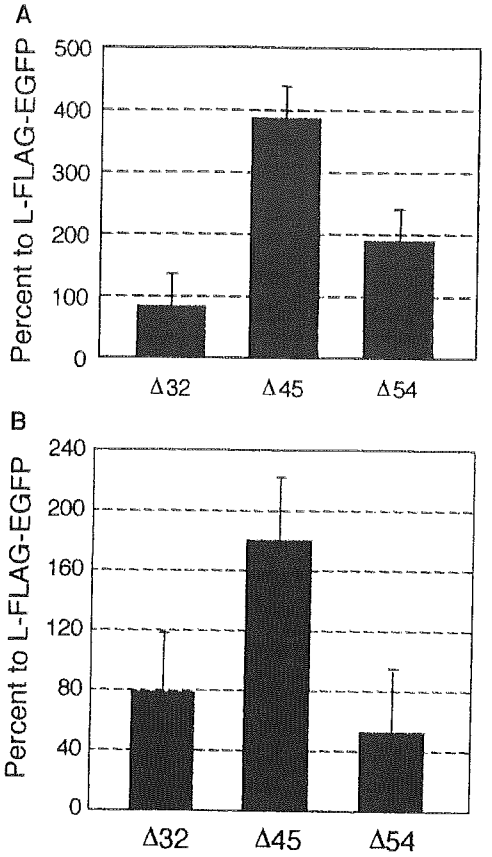

Fig. 3. Secretion of L fusion particles evaluated by enzyme immunoassay and fluorescence. The HBsAg immunoreactivity (A) and the fluorescence (B) in the conditioned medium of the transfected Cos7 cells were measured and the percentages were calculated with the level of L-FLAG –EGFP expression assumed to be 100%. Δ32, Δ45 and Δ54 denote L(Δ32)-FLAG–EGFP, L(Δ45)-FLAG–EGFP and L(Δ54)-FLAG–EGFP, respectively. Each SD was calculated from three independent evaluations.

L(Δ45)-FLAG–EGFP particles were immunoprecipitated with two different antibodies and treated with proteinase K. Western blots with anti-GFP IgG showed two digested EGFP bands of I and II (Fig. 5A) when immunoprecipitated with anti-S IgG, but only one band of II when immunoprecipitated with anti-GFP IgG. The only difference between these two bands of I and II should be due to the size of N-terminal sequence of EGFP protected from proteinase K. This result indicates that the C-terminus of the L-EGFP fusion protein may exhibit dual topology. Because an anti-S IgG recognizes the immunodominant a-epitope, which is common to all six genotypes of HBV as the major surface region of the HBsAg envelope protein [21,22], this antibody will immunoprecipitate all of the L(Δ45)-FLAG–EGFP particles. By contrast, anti-GFP IgG selectively immunoprecipitate particles that display the EGFP moiety at the C-terminus on their surface. With the immunoprecipitates, the EGFP moiety was processed to band II, the N-terminus of which was not protected from proteinase K (Fig. 5A). Anti-S IgG immunoprecipitates included another topology, which protects the N-terminus of the EGFP moiety from proteinase K. There is no

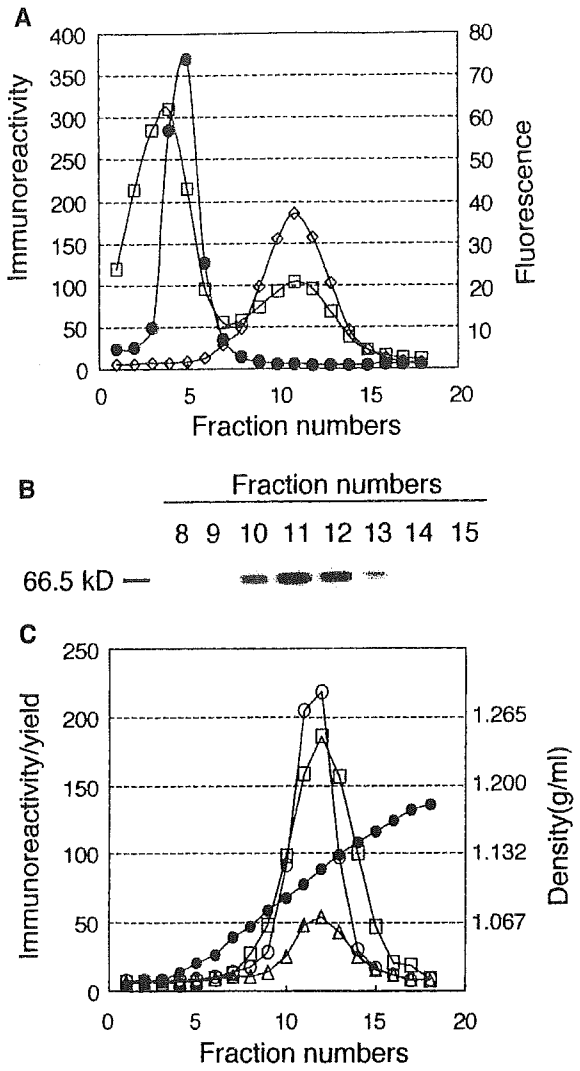

Fig. 4. Particle formation of L(Δ45)-FLAG–EGFP evaluated by sucrose gradient ultracentrifugation. (A) Cell extracts of the Cos7 cells transfected with L(Δ45)-FLAG–EGFP were subjected to sucrose gradient ultracentrifugation and each fraction was evaluated for immunoreactivity (◇) and fluorescence (□). Native EGFP was subjected to centrifugation and the fluorescence from EGFP was simultaneously monitored (●). (B) Fractions that showed both immunoreactivity and fluorescence in (A) were analyzed by western blotting with anti-S IgG. (C) L(Δ45)-FLAG–EGFP particles prepared from conditioned medium (open triangle) and cell extracts [fraction 11 in (B); □] were compared with the BNC prepared from recombinant yeast [6] (○) for immunoreactivity. The density of each fraction was plotted by ●.

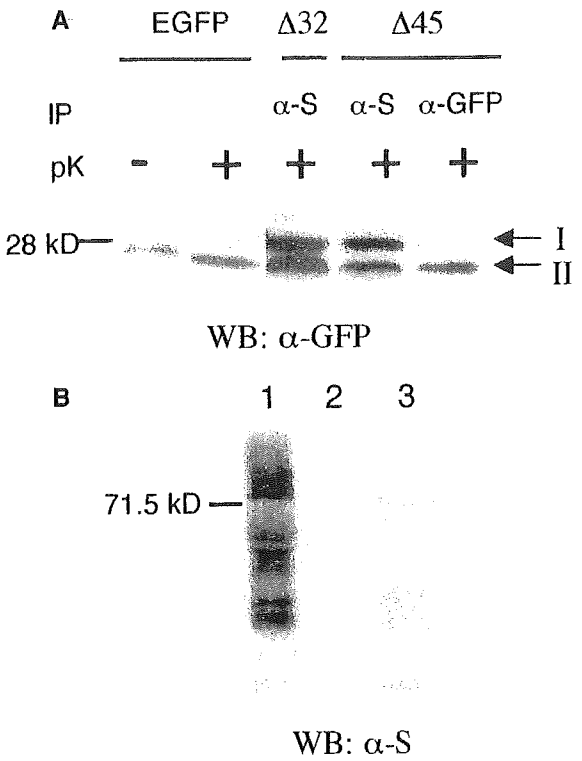

Fig. 5. Evaluation of the C-terminal orientation of the EGFP moiety in L fusion particle. (A) Two different L fusion particles were immunoprecipitated by either anti-S or anti-GFP IgG, and the immunoprecipitates were treated by proteinase K (pK). Δ32 and Δ45 denote L(Δ32)-FLAG–EGFP and L(Δ45)-FLAG–EGFP, respectively. Digested products were detected with anti-GFP IgG. The produced bands were indicated by arrows with I (28 kDa) and II (25 kDa). The native EGFP was treated with or without proteinase K and shown as the reference. In (B) the conditioned medium containing L(Δ45)-FLAG–EGFP particles was immunoprecipitated by anti-GFP IgG (lane 1), and the process was repeated until no L fusion protein could be detected by anti-S IgG (lane 2). The residual supernatant was immunoprecipitated by anti-S IgG (lane 3).

possibility that the dual C-terminal topologies coexist in a particle. However, there should be two types of L(Δ45)-FLAG–EGFP particles, because EGFP moiety-displaying particles immunoprecipitated with anti-GFP IgG showed only single digested product band II. If the two types of C-terminal topology coexist in a particle there should be two digested bands following immunoprecipitation by anti-GFP IgG, as revealed by the anti-S IgG. Thus, we concluded that the EGFP moiety was protected from proteinase K by the membrane when it was located inside the particle, and that it was slightly digested when located on the external side of a particle without membrane protection.

To confirm this finding, we subtracted the L(Δ45)-FLAG–EGFP particles from the conditioned medium with anti-GFP IgG and protein G conjugated to agarose by immunoprecipitation. The residual supernatant was subjected to repeated immunoprecipitation using the same procedure until the L fusion protein could not be detected by western blotting. When the

final subtracted fraction of the supernatant was further immunoprecipitated with the anti-S IgG conjugated to a microparticle, the L fusion protein band was still detected in the fraction, thereby indicating the presence of L fusion particles, which contained EGFP moieties inside (Fig. 5B).

Human hepatocyte specific delivery of EGFP by infection

The preS1 peptide displayed on the surface of L particles recognizes the specific receptor present on human hepatocytes and is essential for HBV infectivity [7,8]. This specific infectivity of the L particle should be independent of the tolerable C-terminus truncation. Cell type-specific infection of L(Δ45)-FLAG–EGFP particles was assessed on various human cancer cells (Fig. 6). After 9 h of incubation with L(Δ45)-FLAG–EGFP particles, EGFP fluorescence was specifically observed in human hepatocellular carcinoma HepG2 cells and NuE cells, whereas no EGFP fluorescence was observed from either human colon adenocarcinoma WiDr cells or human epidermoid carcinoma A431 cells (Fig. 6A). The EGFP fluorescence was not observed in HepG2 cells when incubated with BNC, EGFP or a mixture of BNC and EGFP (Fig. 6B).

Discussion

In this study we attempted to establish a nanocapsule that efficiently delivers protein for tissue- or cell-type-specific targeting. Based on our technology of BNC as a delivery vector, we used a fusion strategy that ensures that the protein of interest is produced as a component of the particle. The fusion proteins between L protein and EGFP (L-FLAG–EGFP) were expressed with or without C-terminal truncation of L protein. It was necessary to truncate the C-terminus of the L protein by 45 amino acids for it to be efficiently secreted from the cells. A EGFP moiety fused to the C-terminus of the L protein appears to prevent secretion, although the mechanism is not currently clear. However, incorrect folding of each half moiety of the fusion protein does not explain the low secretion, because we were able to prepare the particle from both conditioned media and cell extracts. Once prepared,

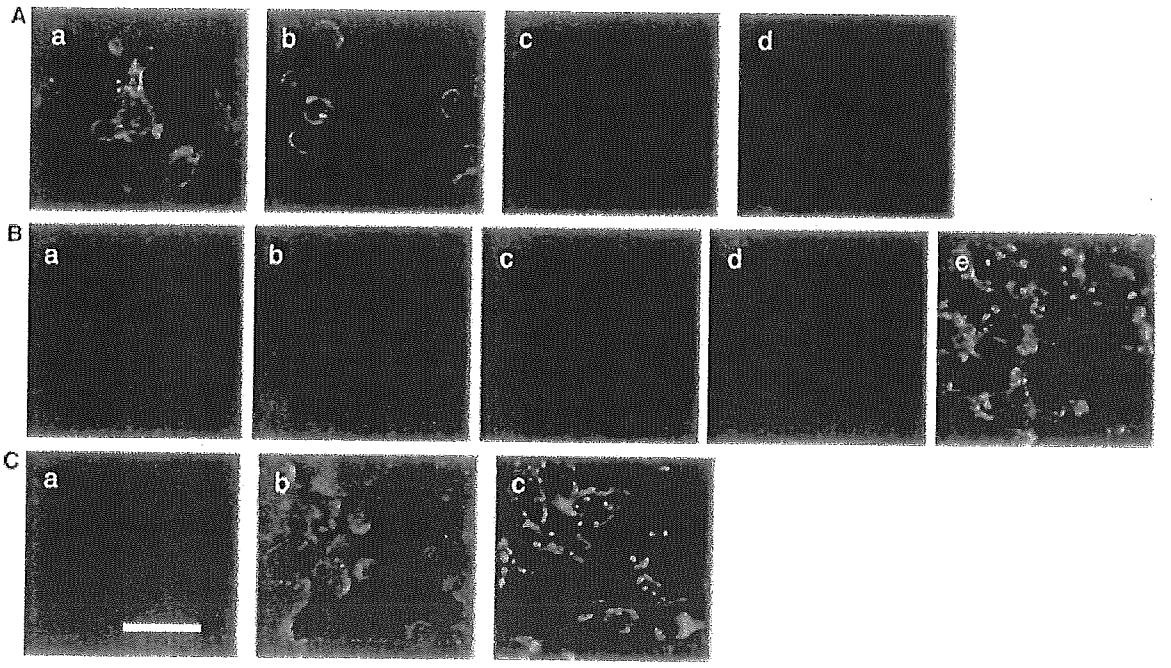

Fig. 6. Infection of L fusion particles *in vitro*. (A) Five nanograms of L(Δ45)-FLAG-EGFP particles obtained from the conditioned medium were added to the culture media of 5×10^4 cells of HepG2 (a), NuE (b), WiDr (c) and A431 (d), respectively. (B) Conditioned medium of nontransfected Cos7 cell (a), 5 ng of BNC from the conditioned medium (b), 100 ng of EGFP (c) and a mixture of 5 ng of BNC with 100 ng of EGFP (d), and 5 ng of L(Δ45)-FLAG-EGFP particles from the conditioned medium (e) were added to 5×10^4 cells of HepG2, respectively. (C) Extracts of nontransfected Cos7 cells (a), 5 ng of L-FLAG-EGFP particles from the extracts of transfected Cos7 cells (b) and 5 ng L(Δ45)-FLAG-EGFP particles from the extracts of transfected Cos7 cells (c) were added to 5×10^4 cells of HepG2. The fluorescence was observed under a confocal microscope at a 63-fold magnification after 9 h infection. Scale bar = 50 μm.

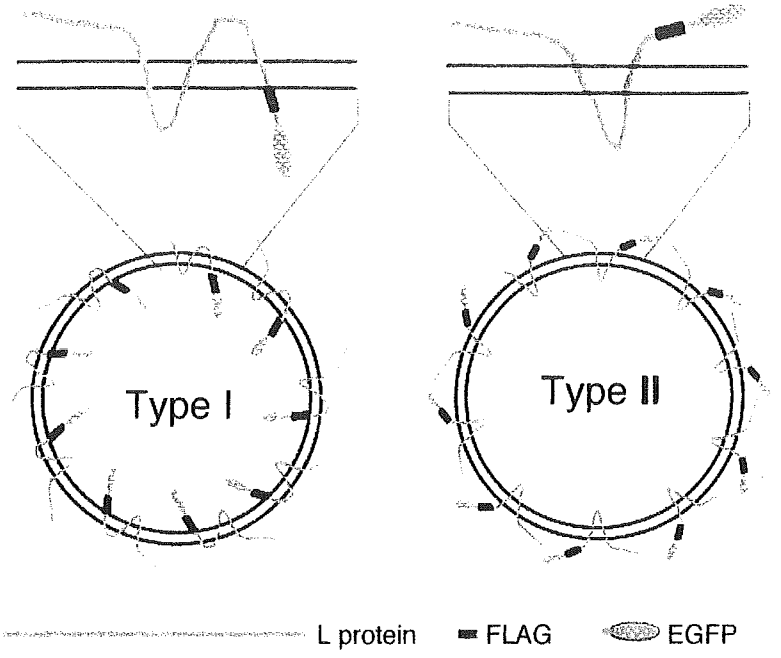

Fig. 7. Proposed models of L fusion particles. Type I, EGFP incorporating particle. Type II, EGFP displaying particle.

particles displayed immunoreactivity in an enzyme immunoassay consistent with the fluorescence intensity, when kept for 3 weeks at 4 °C in the presence of phenylmethanesulfonyl fluoride (PMSF). Furthermore, the cell extract was able to directly infect HepG2 cells (Fig. 6C). These results indicate that the L-FLAG–EGFP particle is stable, if properly prepared, and has the potential to infect cells.

Following optimization of the C-terminal truncation, we attempted to determine the topology of the fused protein in the particle because the purpose of this study was to design a nanoparticle that incorporated a foreign protein using a fusion strategy. One of the purposes of inserting a FLAG-tag between the C-terminus of the L protein and EGFP was to study the topology of the fused protein because we expected enterokinase to specifically recognize and cleave FLAG peptide. Unexpectedly, this protease cleaved other basic residues in the L protein moiety, displaying many degraded products, which confused us. By contrast, the strong resistance of EGFP to proteinase K was extremely useful in studying the C-terminal topology of L fusion protein. Proteinase K treatment of the L(Δ32)-FLAG–EGFP particles showed results similar to those obtained with the L(Δ45)-FLAG–EGFP particle. The hydrophobic sequence of approximately 20–30 amino acids in the C-terminus of the L(Δ32) or L(Δ45) protein may traverse the membrane of lipid bilayer. However, our results show that this terminus is not sufficiently hydrophobic to anchor the C-terminus in the membrane, although it is sufficient to exhibit dual topology. Based on the results of the proteinase K protection assay, we proposed a model of the nanoparticle of L fusion protein (Fig. 7). We designated the particle, whose N-terminal EGFP moiety was incorporated within the membrane, as type I, whereas type II denotes the EGFP moiety displayed on the surface of the particle. Because the particle membrane protected the N-terminal part of the EGFP moiety, proteinase K digestion of type I showed the EGFP moiety to have a slightly higher molecular mass than that produced by the treatment of type II. We scanned the western blots in Fig. 5A and analyzed the densities of the two bands. We found the ratio of band I to band II was 39 : 61. To confirm this ratio, we also compared the immunoreactivity of the conditioned medium containing both type I and type II particles with that of the type II-subtracted medium by the anti-GFP IgG, as shown in Fig. 5B. The ratio of the result is 100 – 36, which means that the ratio of type I to type II is 36 : 64. These different procedures used to estimate the ratio of the particles in two topologies lead to almost equal results. Therefore, we concluded that nearly 40% of the particles are type I. The secretion enhanced by C-terminal truncation might be explained by the fixed topology because we could not detect a particle with a mixed type I and type II topology in one particle. However, it is difficult to find a determinant of the topology of the C-terminal moiety that causes it to be incorporated inside or displayed outside. This unfixed

pattern of topology might clarify the results of previous studies of the topology of the HBsAg protein. It is suggested that the C-terminus of the envelope protein protrudes from the particle in 1987 [12]. Localization of HBV epitope by monoclonal antibodies revealed that the residues 178–186 of the S peptide are exposed on the surface of the virion particle [23]. Kuroda *et al.* described that Asn146 was not glycosylated when the recombinant L particle was prepared from yeast, whereas it was glycosylated when expressed in mammalian cells [3]. This suggests that this aspargine residue is located at the border of the external region and the membrane-bound region. The C-terminal sequence of 56 amino acids from 170 to 226 may be long enough to traverse the membrane twice, although the hydrophobicity is not sufficient to explain the topology precisely. It may be possible to design the C-terminal region as the clear transmembrane region by replacing it with one of the transmembrane-type receptors to limit the topology of the particle to type I.

Our BNC has the same tissue-specific infectivity as HBV because of the N-terminal region of L protein, preS1, which determines its narrow host range and distinct organ tropism. The region from 3 to 77 amino acid residues of preS1 is essential for this specificity [24]. To avoid impairing this selectivity, we fused EGFP to the C-terminal of L protein, which was successfully truncated in order to be secreted from mammalian cells and assembled to an L fusion particle.

We previously reported that BNC containing DNA of interest yielded a very high transfection efficiency with a high specificity of gene transfer to human liver-derived cells [6]. The L fusion particle described here should have equivalent specific transfection efficiency due to the character of the preS1 region of the L protein. The advantage of the fusion particle is that there is no need to incorporate proteins using specialized methods, such as electroporation, for which it is difficult to establish the efficiency needed to transfer genes and drugs into cells. Depending on the cell type, conditions vary and optimization of the conditions may sometimes lead to a 10-fold increase in efficiency. This was also the case with our BNC, and we had to optimize the electroporation conditions, depending on the substances to be incorporated. An efficient procedure is required to eliminate empty particles after electroporation in order to attain the highest efficiency. As for the L fusion particle, all of the particles are destined to convey the protein of interest with a transfection efficiency of nearly 100% directed to human-derived liver cells.

The L fusion particles designed in this study were found to have dual C-terminal topologies, which could easily be separated using antibodies. There was no difference in specific infectivity among them when monitored using EGFP fluorescence (data not shown). This means that it is possible to choose various proteins for the C-terminal moiety of the L fusion proteins, depending on the character of the proteins to be fused. This possibility will include cytoplasmic proteins, as well as cytokines or ligands, for the cell surface. In this context, one of the candidates of the moiety might be interferon (IFN) which is used with ribavirin to treat hepatitis C virus-induced liver disease. This therapy has many does-dependent side effects, such as depression and insomnia. The L–IFN fusion particle would be extremely useful because it targets only the liver so that the dose administered could be low so that the side effects would not be a cause for concern.

Retargeting of BNC by replacing the preS1 region with other targeting moieties or biorecognition molecules, such as ligands, receptors and antibodies as previously proposed [6], should also be applicable to the L fusion particles. The greatest problem in using the particle is that people who have antibodies to HBV are increasing in number due to the widespread hepatitis B vaccination program. Stealth mutations at Gln129 and Gly145 to Arg would not only address this problem, but also lead to a design of the delivery vector with extremely low immunogenicity [25,26]. Thus, we are developing our BNC for its potential to become a practical vector of protein delivery.

Experimental procedures

Cell cultures

Human hepatoma HepG2 cells, human squamous cell carcinoma A431 cells and human colon adenocarcinoma WiDr cells were cultured in Dulbecco's modified Eagle medium (DMEM), supplemented with 10% (v/v) fetal bovine serum (FBS; PAA Laboratories, Pasching, Austria). Human hepatoma NuE cells were cultured in RPMI-1640 with 10% (v/v) FBS. African green monkey kidney-derived Cos7 cells for particle production were maintained in DMEM supplemented with 5% (v/v) FBS. These cells were maintained at 37 °C/5%CO_2.

Construct of plasmids

The HBV L gene was excised from the plasmid pGLD LIIP39-RcT [7] and inserted into the *Xho*I site of pEGFP-N1 vector (Clontech, Mountain View, CA). Then the synthetic oligo-nucleotide coding FLAG-tag sequence (5′-ATATATTGATTACAAGGATGACGACGATAAGA TA-3′) was inserted between the *Acc*I site close to the C-terminus of the L protein and the *Age*I site at the N-ter-